Article

Evaluation of the Impacts of Change in Land Use/Cover on Carbon Storage in Multiple Scenarios in the Taihang Mountains, China

Huanchao Guo, Shi He *, Haitao Jing, Geding Yan and Hui Li

School of Surveying and Land Information Engineering, Henan Polytechnic University, Jiaozuo 454000, China; 212104010006@home.hpu.edu.cn (H.G.); jht@hpu.edu.cn (H.J.); 212104020020@home.hpu.edu.cn (G.Y.); 212104010008@home.hpu.edu.cn (H.L.)
* Correspondence: heshi@hpu.edu.cn

Abstract: Research on the spatiotemporal changes in land use/cover (LUC) and carbon storage (CS) in the region of the Taihang Mountains in various developmental scenarios can provide significant guidance for optimizing the structure of LUC and formulating ecologically friendly economic development policies. We employed the PLUS and InVEST models to study change in LUC and CS in the Taihang Mountains from 1990 to 2020. Based on these results, we established three distinct development scenarios: a business-as-usual development scenario, a cropland protection scenario, and an ecological conservation scenario. Based on these three developmental scenarios, we simulated the spatiotemporal changes in LUC and CS in the Taihang Mountains in 2035. The results indicate that: (1) from 1990 to 2020, the CS in the Taihang Mountains increased from 1575.91 Tg to 1598.57 Tg, with a growth rate of approximately 1.44%. The primary source of this growth is attributed to the expansion of forests. (2) In the business-as-usual development scenario, the growth rate of CS in the Taihang Mountains was approximately 0.45%, indicating a slowdown in the trend. This suggests that economic development has the consequences of aggravating human–land conflicts, leading to a deceleration in the growth of CS. (3) In the cropland protection scenario, the increase in the CS in the Taihang Mountains was similar to the CS increase in the business-as-usual development scenario. However, the expansion of cropland dominated by impermeable surfaces, which indicates economic development, was considerably constrained in this scenario. (4) In the ecological conservation scenario, the increase in carbon storage in the Taihang Mountains was 1.16%, which is the fastest among all three scenarios. At the same time, there was a certain degree of development of impermeable surfaces, achieving a balance between economic development and ecological conservation.

Keywords: PLUS model; InVEST model; land use/cover change; carbon storage; scenario simulation

1. Introduction

Global climate change represents one of the most pressing challenges facing contemporary human society, having profound ramifications for the sustainability of human economic and social development [1–3]. Since the onset of the industrial revolution, human society has progressively embarked on a path of modernization. However, within this process, the extensive combustion of fossil fuels, such as coal [4] and petroleum, has resulted in a substantial release of greenhouse gases, such as carbon dioxide (CO_2) into the atmosphere [5]. Simultaneously, population growth [6] and urban expansion [7] have diminished the capacity of terrestrial ecosystems to absorb CO_2 from the atmosphere. In response to global climate change, the international community has undertaken substantial efforts, exemplified by conventions and agreements such as the United Nations Framework Convention on Climate Change (UNFCC), the Kyoto Protocol, and the Copenhagen Accord [8]. These initiatives underscore the crucial role of terrestrial ecosystems, particularly

forests, as vital carbon reservoirs [9–12], thereby profoundly propelling the international community's endeavor to address global climate change.

As the world's largest developing country, China has experienced rapid economic growth in recent decades [13,14]. However, due to its rough approach on economic development, low resource productivity, inadequate governmental regulatory capacity, and the limited environmental awareness among the public, China's natural ecological environment has suffered significant degradation [15,16]. At present, environmental issues have become a major concern that the Chinese government must address [2,17]. The simulation and analysis of carbon storage in ecosystems and its future changes can assist governmental decision-making bodies in accurately understanding trends in the variations in local ecosystem carbon storage [18,19], thereby achieving the dual objectives of economic development and environmental protection [20–22].

Changes in LUC are tangible manifestations of anthropogenic activities transforming the natural environment [23,24]. Changes in land use have direct impacts on carbon stocks. The authors of [25] conducted a study on land use and soil carbon sequestration in the United Kingdom, revealing that 95% of carbon sequestration is influenced by changes in land use. The authors of [26] conducted research on carbon stocks in southwestern Rwanda which showed that transitions from annual crops to plantation forests led to an increase of 193%, while clearing forests for agricultural purposes resulted in a loss of 72%. A quantitative analysis of the relationship between changes in land use and carbon storage and a planned adjustment of the structure of LUC can be conducive to guiding the development of a low-carbon economy [21–24,27]. Traditional prediction models like Markov models, system dynamics (SD) models, and cellular automata (CA) models apply only to specific scales or characteristics [20]. The PLUS model constitutes a cellular automaton model rooted in multi-type random patch seeds, and it incorporates a land expansion analysis strategy (LEAS). Through its implementation, the PLUS model attains heightened accuracy in the simulation and prediction of changes in LUC [28]. It finds extensive application in current research on changes in LUC [29,30]. The Integrated Valuation of Ecosystem Services and Tradeoffs (InVEST) model serves as a tool to explore the impact of ecosystem changes on benefits to human society [31,32]. It is one of the most widely used models in current CS change studies. By utilizing the InVEST model, carbon storage information can be derived from land use data. Researchers have conducted numerous studies on changes in land use, land cover, and carbon storage in multiple regions [33–35]. Some have examined the effects of changes in LUC on CS in arid areas [36] and Hainan Island [37] of China. Others have evaluated changes in LUC and CS under different climate change scenarios [38]; the authors of [39] researched changes in LUC and CS in the coastal area of Shandong Province from 2000 to 2020, providing simulations for 2030. The authors of [40] conducted a study on changes in LUC in the Yellow River Basin from 2000 to 2040 and their impact on CS. In general, distinct variations exist in the carbon sequestration capacities of different types of LUC, and the conversions between various types of LUC directly influence the CS in the study area. It is widely acknowledged that natural ecological types of LUC, such as forests, croplands, wetlands, and grasslands, play crucial roles in augmenting the CS within a study area [27,41–44]. However, in research on arid regions, the expansion of cropland was primarily dominated by high-carbon-density forest and wetland, leading to a decline in the overall CS across the entire study area [36]. Furthermore, built-up areas exhibit lower carbon densities, resulting in weaker carbon absorption capacities for CO_2, consequently leading to reduced regional CS [45,46]. To realize an increase in CS, measures may be taken to control economic and population growth while expediting the transition to renewable energy sources.

The Taihang Mountains serve as the dividing line between the North China Plain and the Loess Plateau, playing a vital role as an important mountain range and geographical boundary in eastern China. In terms of topographical features, the Taihang Mountains are positioned within the transitional region between the first and second tiers of China's topographic landscape. Ecologically, the Taihang Mountains reside within an intricate

ecological transition zone and vegetation shift area [33]. Characterized by an arid climate, limited water resources, a vulnerable soil structure, and a susceptibility to wind and water erosion and anthropogenic activities, the Taihang Mountains exemplify a classic case of an ecologically fragile region [47–49]. Changes in LUC may directly impact the local ecological security pattern and development prospects. Therefore, it is imperative to conduct research on changes in LUC and CS in the Taihang Mountains [50]; this research can provide significant guidance for formulating future development strategies in this region.

Based on the PLUS model, we conducted an analysis of changes in LUC in the Taihang Mountains from 1990 to 2020, in addition to their underlying driving factors, to elucidate the patterns of change in the LUC in the Taihang Mountains. Additionally, we performed simulations to predict the LUC patterns in the Taihang Mountains in 2035 for three different scenarios. Using the InVEST model, we assessed spatiotemporal variations in the CS in the Taihang Mountains, exploring the dynamics of these changes. The objective was to optimize the structure of the LUC in the area, striking a balance between economic development and the quality of the ecological environment, thereby achieving harmonious coexistence between humans and nature in the Taihang Mountains.

2. Materials and methods

2.1. Study Area

The Taihang Mountains ($35°15' \sim 41°00'$ N, $110°14' \sim 116°35'$ E) stand as a natural demarcation between the Loess Plateau and the North China Plain (Figure 1). The Taihang Mountains span four provinces and municipalities: Beijing, Hebei, Shanxi, and Henan. They are located on the eastern edge of China's second geographical tier and serve as a zone of transition from the eastern plains to the central and western mountainous plateaus [33]. The terrain rises in the west and descends in the east, with a continuous chain of mountains and a network of valleys within the region. The mountain range begins in the north at Xi Mountain in Beijing and extends southward to Wangwu Mountain, the boundary area between Henan and Shanxi. To the west, the Taihang Mountains border the Shanxi Plateau, while to the east, they overlook the North China Plain. The total area covers approximately 1.278×10^4 km^2. The primary types of land use in the Taihang Mountains include cropland, forest, grassland, shrub, barren, impervious surface, and water. Among these, cropland, forest, and grassland hold dominant positions [49].

2.2. Data Sources

We utilized the China Land Cover Dataset (CLCD), which was released by Wuhan University [51] and has a spatial resolution of 30 m. Land use data for the years 1990, 2005, and 2020 were selected in order to partition the entire period into two equal periods. This approach enabled us to simulate the changes in land use between 1990 and 2005 to predict the alterations in land use in 2020. Subsequently, the simulated outcomes were contrasted with the actual land use data for 2020, thereby facilitating the validation of the accuracy of the PLUS model's simulation. The study area comprises seven land cover types: cropland, forest, shrub, grassland, water, barren, and impervious surface. Data relating to both social and natural driving factors were collected for this research. The social driving factors comprised the distance to a national road, the distance to a provincial road, the distance to a railway, the distance to a highway, the population density, and the GDP; while the natural driving factors encompassed the distance to a river, temperature, precipitation, DEM, slope, and soil type. The driving force data used in this study were obtained from the Resource and Environment Science Data Center of the Chinese Academy of Sciences (https://www.resdc.cn/) (accessed on 18 February 2023) and OpenStreet Map, with the specific origins detailed in (Table 1). Before inputting the data into the model, all datasets were resampled to a consistent spatial resolution of 30 m, matching the resolution of the land cover data. This approach ensured compatibility and accuracy in the analysis of changes in the LUC in the Taihang Mountains.
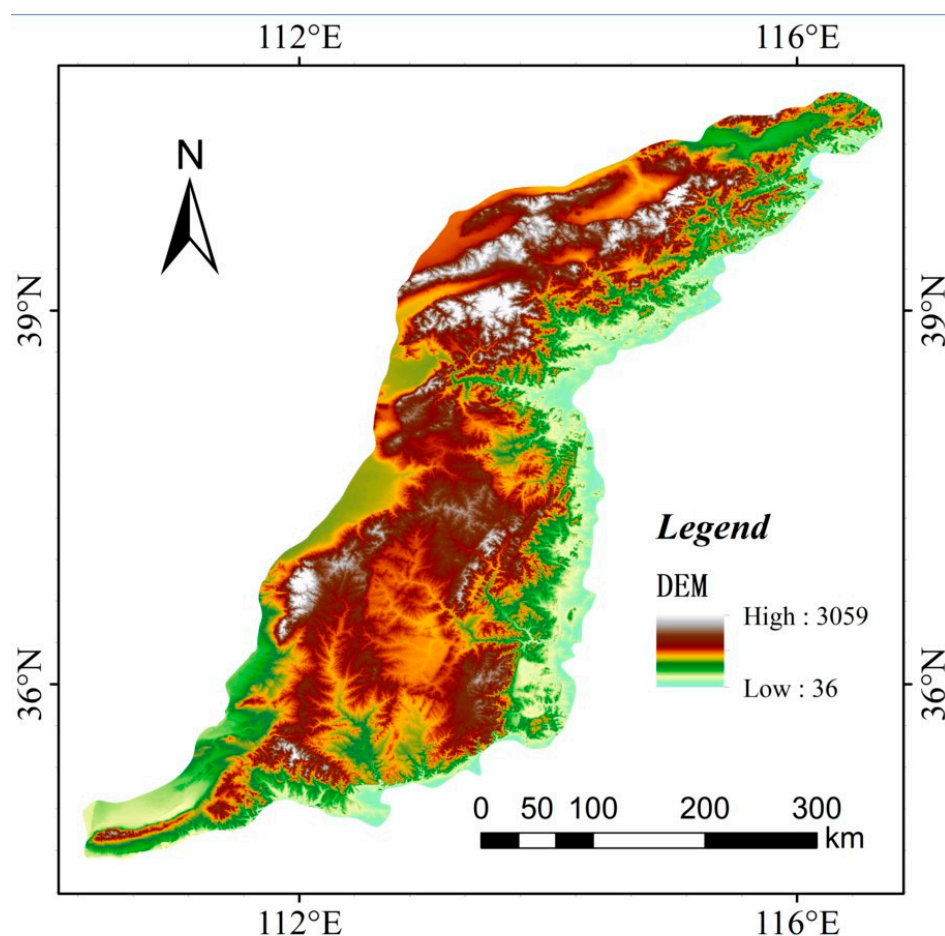
Figure 1. The study area.

Table 1. Data sources.

Data	Data Attribute	Year	Resolution	Sources
LUC	-	1990, 2005 and 2020	30 m	https://zenodo.org
	Distance to national road	2020	30 m	OpenStreetMap
	Distance to provincial road	2020	30 m	OpenStreetMap
Social factor	Distance to railway	2020	30 m	OpenStreetMap
	Distance to highway	2020	30 m	OpenStreetMap
	Population density	2020	1 km	https://www.resdc.cn/
	GDP	2020	1 km	https://www.resdc.cn/
	Distance to river	2015	30 m	https://www.resdc.cn/
	Temperature	2015	250 m	https://www.resdc.cn/
	Precipitation	2015	1 km	https://www.resdc.cn/
Natural factor	DEM	2015	30 m	https://www.resdc.cn/
	Slope	2015	30 m	https://www.resdc.cn/
	Soil type	2010	1 km	https://www.resdc.cn/

2.3. Method

2.3.1. The PLUS Model

Cellular automata (CA) are widely applied to simulate complex changes in the LUC. The PLUS model integrates rule-mining methods based on land expansion analysis strategy (LEAS) and a CA model based on multi-type random patch seeds (CARS). The LEAS employs a random forest algorithm to uncover the underlying causes of changes in the LUC. Utilizing the LEAS, we can unveil expansion patterns for all types of LUC and determine the contribution of each driving factor to the expansion of each type of LUC.

The calculation can be expressed as follows (1). The CA model is a scenario-driven land use simulation model which leverages multi-type random patch seeds. CARS enables the simulation of changes in LUC from a macroscopic scale down to a microscopic scale. The calculation can be expressed as follows (2). The PLUS model is capable of identifying the driving factors of land expansion and predicting the patch-level evolution of land use landscapes [52].

$$P_{i,k}^d(x) = \frac{\sum_{n=1}^{M} I(h_n(x) = d)}{M} \tag{1}$$

where $P_{i,k}^d(x)$ represents the growth probability of land use type k at cell i; the value of d equals 0 or 1, while $d = 1$ represents other land use types changes to land use type k and $d = 0$ represents other transitions; x is a vector that consists of multiple driving factors; $I(\cdot)$ is the function of the decision tree set; $h_n(x)$ is the prediction type of the n-th decision tree for vector x; M is the total count of decision trees.

$$OP_{i,k}^{d=1,t} = \begin{cases} P_{i,k}^{d=1} \times (r \times \mu_k) \times D_k^t \ if \ \Omega_{i,k}^t = 0 \ and \ r < P_{i,k}^{d=1} \\ P_{i,k}^{d=1} \times \Omega_{i,k}^t \times D_k^t \ all \ others \end{cases} \tag{2}$$

where $OP_{i,k}^{d,t}$ represents the overall evolution probability of land use type k; r is a random value which varies from 0 to 1; μ_k represents the threshold values to generate new land use type k; D_k^t represents the future demand impact of land use type k which depends on iterating out the gap between the quantity and demand in year t; $\Omega_{i,k}^t$ represents the neighborhood effects about land use type k at cell i.

We established the three following distinct development scenarios [46]:

Scenario A: the business-as-usual development scenario. Based on trends in the LUC in the Taihang Mountains from 1990 to 2020, a scenario was constructed to simulate the business-as-usual development of LUC from 2020 to 2035.

Scenario B: the cropland priority scenario. Considering China's cropland protection policies and the need to maintain a certain area of cropland within the study area, this scenario was designed to prioritize cropland protection. In this scenario, conversions of cropland to other types of LUC were prohibited, ensuring the preservation of cropland quantity.

Scenario C: the ecological priority scenario. Faced with urgent global challenges such as climate change, resource depletion, and the loss of biodiversity, it is imperative for humanity to take swift action to protect the Earth's ecosystems. In this scenario, conversions of forests, shrubs, grasslands, and water bodies to other types of LUC were prohibited, emphasizing ecological conservation.

These scenarios provide different perspectives on changes in LUC, allowing for an assessment of their potential impacts and implications in the contexts of various development priorities and environmental considerations (Table 2).

Table 2. The rule matrix of LUC conversion in three scenarios (a—cropland; b—forest; c—shrub; d—grassland; e—water; f—barren; g—impervious surface).

	Scenario A							Scenario B							Scenario C						
	a	b	c	d	e	f	g	a	b	c	d	e	f	g	a	b	c	d	e	f	g
a	1	1	0	1	0	0	1	1	0	0	0	0	0	0	1	1	0	1	0	0	1
b	1	1	0	0	0	0	0	1	1	0	0	0	0	0	0	1	0	0	0	0	0
c	1	1	1	1	0	0	0	1	1	1	1	0	0	0	1	1	1	0	0	0	0
d	1	1	1	1	0	0	0	1	1	1	1	0	0	0	1	1	1	0	0	0	0
e	1	0	0	0	1	0	1	1	0	0	0	1	0	1	0	0	0	0	1	0	1
f	1	0	0	1	1	1	1	1	1	0	0	1	1	1	1	1	1	0	1	1	1
g	0	0	0	0	0	0	1	0	0	0	0	0	0	1	0	0	0	0	0	0	1

2.3.2. LUC Transition Matrix

The LUC transition matrix serves as a valuable tool for illustrating the internal transitions in LUC within a region over a specified period of time. This method is derived from the quantitative description of the system state and state transitions in system analysis. Within the LUC transition matrix, each row represents a type of LUC at time t_1, while each column represents a type of LUC at time t_2. The element A_{ij} signifies the area transitioning from LUC type i to type j between time t_1 and t_2, and the element A_{ii} represents an area in which the LUC remains unchanged from time t_1 to t_2. The mathematical expression of the LUC transition matrix is as follows (3):

$$A_{ij} = \begin{bmatrix} A_{11} & A_{12} & \dots & A_{1n} \\ A_{21} & A_{22} & \dots & A_{2n} \\ \dots & \dots & \dots & \dots \\ A_{n1} & A_{n2} & \dots & A_{nn} \end{bmatrix} \tag{3}$$

2.3.3. InVEST Model

The InVEST model is designed to offer informational support for decision making in natural resource management. It furnishes insights into how potential changes in relevant ecosystems can lead to alterations in the flow of benefits to humanity [27,32]. The InVEST model typically employs a production function approach to quantitatively assess ecosystems. Specifically, concerning carbon storage, InVEST computes carbon storage using the following formula:

$$C_i = C_{above} + C_{below} + C_{soil} + C_{dead} \tag{4}$$

$$C_{total} = \sum_{i=1}^{n} A_i C_i \tag{5}$$

where i denotes the LUC type; n represents the total number of types of LUC; C_i denotes the total carbon density of a LUC type i; C_{above}, C_{below}, C_{soil}, and C_{dead}, respectively, represent the carbon density of the aboveground biomass, belowground biomass, soil, and dead matter for the land use type i; A_i represents the area of the LUC type i; and C_{total} denotes the total CS of the terrestrial ecosystem.

The carbon density data we used were based on previous research [36,38–40]. Considering that data for the carbon density of dead matter are challenging to obtain and that it constitutes a relatively small proportion of the overall carbon storage, the current study did not take it into account. Table 3 presents the final carbon density data for each LUC type within the study area.

Table 3. Carbon density of each LUC type (t/ha).

	C_{above}	C_{below}	C_{soil}
Cropland	1	14.5	79.5
Forest	7.6	20.8	158.8
Shrub	6.5	12.4	100.7
Grassland	6.3	15.5	86.9
Water	0.5	0	0
Barren	0.2	0	21.6
Impervious surface	0.4	0	0

2.3.4. Spatial Autocorrelation

According to the First Law of Geography, neighboring objects tend to exhibit greater similarities and interactions than distant objects, a concept known as "spatial dependence". Spatial autocorrelation refers to the degree of spatial dependence between the observed values of a spatial entity and the values of the same variable for neighboring observations [53]. Moran's I is commonly used for calculating spatial autocorrelation [54]. Moran's I can be

divided into the global Moran's I and the local Moran's I, representing the overall spatial autocorrelation and the local autocorrelation, respectively. The computation of Moran's I is as follows:

$$I = \frac{\sum_i \sum_j w_{ij} z_i \cdot \frac{z_j}{S_0}}{\sum_i \frac{z_i^2}{n}} \tag{6}$$

$$z_i = x_i - \overline{x} \tag{7}$$

where w_{ij} denotes the spatial weight matrix; x_i denotes the observation at location i; $\overline{x}$ is the mean of the variable x; $S_0 = \sum_i \sum_j w_{ij}$ denotes the sum of all spatial weight matrixes; and n denotes the total number of spatial units. The value of Moran's I ranges from -1 to 1 in which [0, 1] indicates a positive spatial correlation among geographic entities, and $[-1, 0]$ indicates a negative spatial correlation. Values closer to 0 suggest a weaker spatial correlation among geographic entities, tending toward a random distribution.

In a practical application, a Moran's I scatterplot is often generated to visually analyze the spatial heterogeneity of data. In the scatterplot, the first quadrant represents a high–high cluster, indicating that the geographic entities are both high in value and are surrounded by high-value neighbors; the second, third, and fourth quadrants, respectively, represent low–high, low–low, and high–low clustering.

The Moran's I scatterplot can only provide a preliminary assessment of the spatial heterogeneity of geographic entities as a whole. It cannot determine the local correlations of different regions or whether clustering areas are statistically significant. Therefore, it is necessary to utilize local indicators of spatial association (LISA) cluster maps to further analyze the local spatial heterogeneity of geographic entities [55].

3. Results

3.1. Changes in LUC

3.1.1. The Impact of Driving Factors

Changes in LUC are frequently influenced by a number of factors. Utilizing the land expansion analysis strategy (LEAS) of the PLUS model, we assessed the impacts of the selected six social factors and six natural factors on the variations in the types of LUC across the region of the Taihang Mountains. Ultimately, this analysis yields the contribution of each driving factor to the expansion of each type of land use (Figure 2). These driving factors serve as crucial support for the subsequent simulation of changes in the LUC in the Taihang Mountain.

3.1.2. Changes in the LUC: 1990–2020

A transition matrix for the changes in the LUC for the years 1990–2020 was calculated using the LUC data in the Taihang Mountains from 1990–2020 (Table 4 and Figure 3). Cropland, forest, shrubs, grasslands, water, barren, and impervious surface comprised, respectively, 38.7%, 28.8%, 1.5%, 27.0%, 0.4%, 0.005%, and 2.5% of the total area in 1990. These percentages changed to 33%, 33.4%, 1%, 26%, 0.4%, 0.004%, and 4.8%, respectively, by the year 2020. It is clear that cropland, forest, and grassland account for the majority of LUC types in the Taihang Mountain, with a combined proportion of about 90%.

Between 1990 and 2020, cropland and shrub areas exhibited noticeable declining trends. Cropland experienced the most pronounced reduction; approximately 7171.2 km^2 of cropland was lost over the 30-year period, accounting for about 14.4% of the total cropland area in 1990. This constitutes the largest decrease in the Taihang Mountains over the past three decades. Shrub areas declined by a total of 460.4 km^2, representing about 25.1% of the shrub area in 1990, making it the most significant proportional decrease in the Taihang Mountains over the last thirty years. Conversely, forest and impervious surface exhibited evident growth trends. Forest areas expanded by a net area of 5972.1 km^2, representing the largest increase among all types of LUC, and impervious surface expanded by a net area of 3068.6 km^2, accounting for about 96.5% of the impervious surface area in

1990 and representing the highest growth rate among all types of LUC. Grassland, water, and barren remained stable with minor fluctuations.

Table 4. The LUC transition matrix of the Taihang Mountain for the period 1990–2020 (km^2).

|		2020							Total
		Cropland	**Forest**	**Shrub**	**Grassland**	**Water**	**Barren**	**Impervious Surface**	**Total**
	Cropland	39,796.479	1605.1104	11.2086	5475.3282	139.932	0.7911	2868.318	49,897.1673
	Forest	464.1012	36,511.6068	171.4806	190.2752	1.1952	0.0189	29.0835	37,367.7614
	Shrub	7.3512	721.1538	613.7208	487.5201	0.0009	0.0189	0.2817	1830.0474
1990	Grassland	2335.5576	4499.0514	473.1993	27,501.3477	9.8145	4.1121	163.8225	34,986.9051
	Water	116.7984	2.8881	0	3.2526	378.9936	0.0018	36.6171	538.5516
	Barren	0.351	0	0	1.3797	0.3528	0.5445	4.4838	7.1118
	Impervious surface	5.3595	0.0837	0	0.3861	28.1934	0.0063	3144.0627	3178.0917
	Total	42,726	43,339.8942	1269.6093	33,659.49	558.4824	5.4936	6246.669	127,805.6
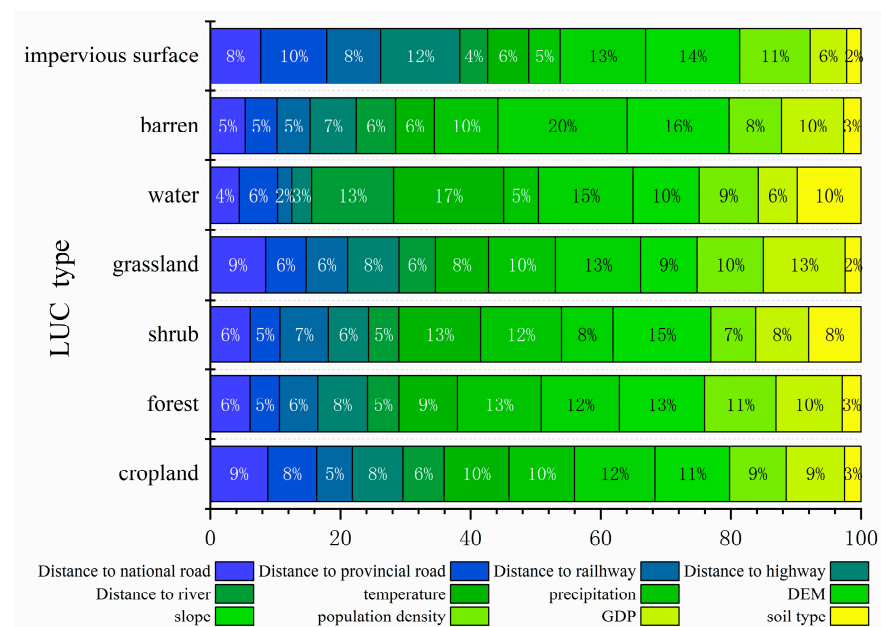
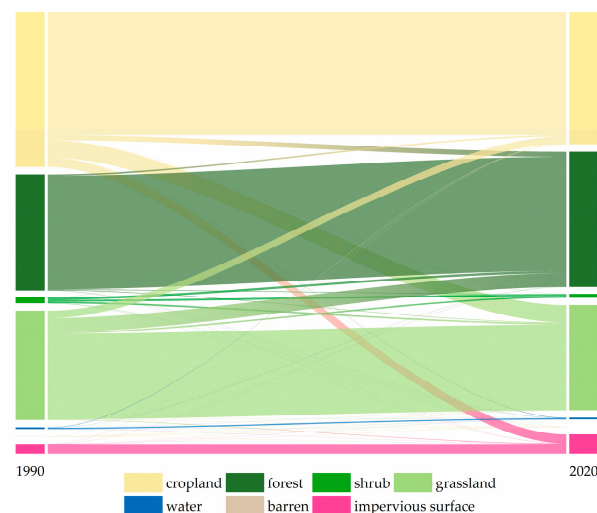**Figure 2.** The contribution of each driving factor to each type of LUC.

Figure 3. Visualization of LUC transition matrix.

3.1.3. Simulation for LUC in 2035

First, the LUC data from 1990 to 2020 were divided into two periods. Based on the LUC data from 1990 to 2005, the PLUS model was used to simulate the LUC pattern for 2020, which was then compared with the actual data for 2020. The results show that the kappa coefficient [56] is 0.86, and the figure of merit (FoM) [52] is 0.35, indicating the high degree of accuracy of the model's simulation and the high level of credibility of its results. Different development scenario parameters were input into the PLUS model to obtain the Taihang Mountains' LUC pattern for 2035 under different development scenarios (Figure 4).
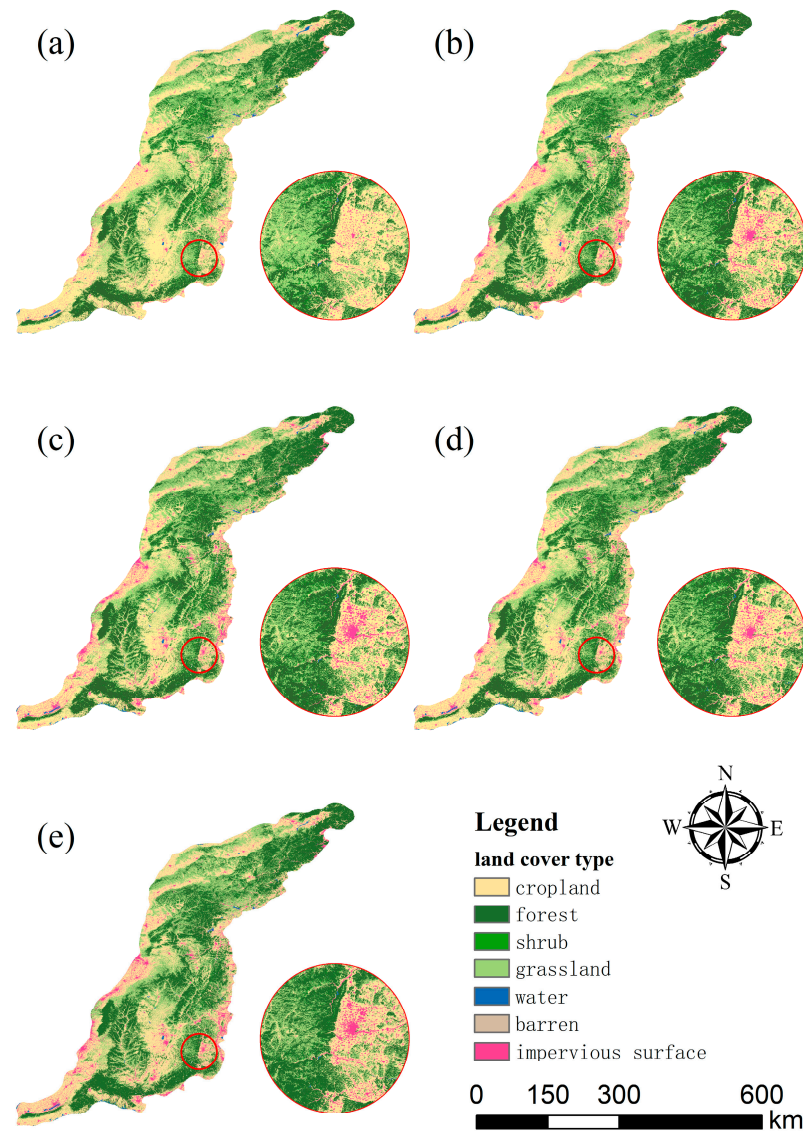
Figure 4. Distribution of LUC in the Taihang Mountains. LUC distribution in (**a**) 1990; (**b**) 2020; (**c**) Scenario A; (**d**) Scenario B; (**e**) Scenario C.

Based on the results of the simulation, in Scenario A, each LUC type will maintain its original trend. Forest demonstrates the highest increase, with a net addition of 1676.09 km^2 which is the largest increase among all types of LUC. Impervious surfaces will experience the highest growth rate, with an 11.85% increase. Cropland will decrease by 1423 km^2, the largest reduction among all the types of LUC. Shrub areas will decline by 16.8%, the highest reduction proportion among all types of LUC. Additionally, the rate of decline in grassland shows a decrease (Table 5).

Table 5. Area of different LUC types under different development scenarios (km^2).

LUC Type	2020	Scenario A	Scenario B	Scenario C
Cropland	42,726	41,302.39	42,976.47	41,252.0638
Forest	43,339.89	45,015.99	44,327.19	45,502.1131
Shrub	1269.609	1055.387	887.9072	1249.4994
Grassland	33,659.49	32,913.34	32,913.34	32,949.33806
Water	558.4824	526.1354	526.1354	544.1353743
Barren	5.4936	5.135654	4.611866	5.23064114
Impervious surface	6246.67	6987.257	6169.984	6303.2576

In Scenario B, cropland has been effectively preserved. Unlike the other two scenarios, the area covered by cropland in the Taihang Mountains shows an increasing trend. Compared to Scenario A, the cropland area increases by 1674.08 km^2 (+3.9%). However, all other types of LUC except for forests exhibit a declining trend. Among them, shrub-covered areas show the most significant decline, with a decrease of 381.7018 km^2 that is primarily concentrated in the central part of the Taihang Mountains. Additionally, impervious surface also experiences a decline which is mainly concentrated on the eastern side of the Taihang Mountains, with few declines observed on the western side. This may be attributed to the relatively developed economy and stronger economic capacity in the eastern part of the Taihang Mountains, enabling a better implementation of cropland protection policies.

In Scenario C, compared to 2020, the overall areas of forest, shrub, grassland, and water increase by 1417.61 km^2 (+1.798%). However, among these categories, only the forested areas expand, while shrubland, grassland, and water experience a certain degree of decline, with reductions of 1.58%, 2.1%, and 2.57%, respectively. Spatially, the decline in shrubs, grassland, and water mainly occurs around the forest, and in terms of attributes, these lands are mostly transformed into forested areas. This indicates that with the improvement of the natural environment, the expansion of the forest will encroach upon the surrounding shrub, grassland, and water. Additionally, there is a slight increase in impervious surface.

3.2. The Change in Carbon Storage

According to the calculations from the InVEST model, the overall CS in the Taihang Mountains was 1575.91 Tg (1 Tg = 10^{12} g) in 1990. By the year 2020, it increased to 1598.57 Tg (+1.44%). Spatially, the Taihang Mountains exhibit a centrally high and peripherally low distribution of CS. In the Taihang Mountains, croplands, forests, and grassland areas contribute to the vast majority of CS, accounting for over 98%. This is the combined result of two factors: firstly, these types of LUC have relatively high carbon densities, and secondly, they are the dominant types of LUC in the Taihang Mountains. In comparison, shrubs have a higher carbon density than cropland. However, due to the smaller coverage of shrublands in the Taihang Mountains, their contribution to the overall CS is relatively low (Table 6).

Table 6. CS values of different LUC types under different development scenarios (Tg).

	Cropland	Forest	Shrub	Grassland	Water	Barren	Impervious Surface	Total
1990	474.02	699.52	21.89	380.31	0.027	0.015	0.13	1575.91
2020	405.9	811.32	15.18	365.88	0.028	0.012	0.25	1598.57
Scenario A	392.37	842.7	12.62	357.77	0.026	0.011	0.28	1605.78
Scenario B	408.28	829.8	10.62	357.77	0.026	0.01	0.25	1606.75
Scenario C	391.89	851.8	14.94	358.16	0.027	0.011	0.25	1617.09

The simulation results for different development scenarios indicate that the overall carbon storage and its spatial patterns in the Taihang Mountains will vary due to differences in the LUC patterns. In all three development scenarios, the overall CS in the Taihang Mountains shows an increasing trend. In Scenario A, the CS is expected to increase by

7.21 Tg (0.45%) by the year 2035. Compared to the period from 1990 to 2020, the increase in CS has decreased, which can be attributed to urban expansion and economic development. This decline underscores the importance of prioritizing ecological and environmental conservation efforts.

Compared to Scenario A, the increase in the coverage of cropland in Scenario B contributes to an additional CS of 2.38 Tg in the Taihang Mountains. Additionally, the expansion of forests provided an additional CS value of 18.48 Tg. At the same time, the CS provided by other types of LUC decreased. Overall, in Scenario B the total CS in the Taihang Mountains increased by 8.18 Tg (+0.51%) (Figure 5).
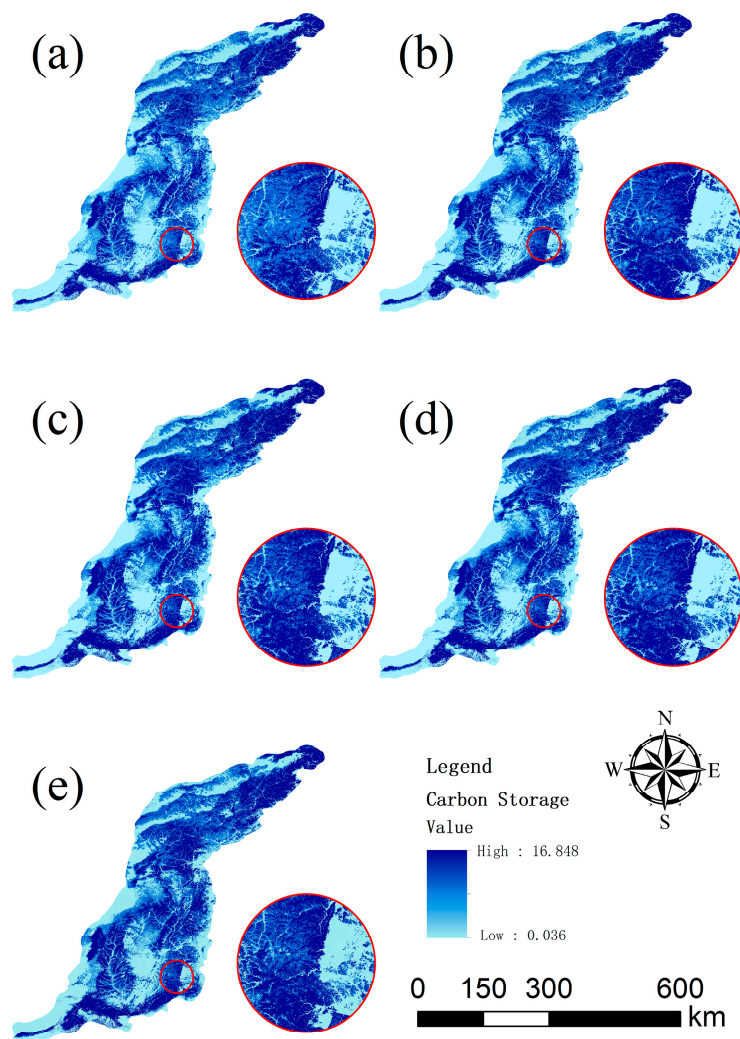
Figure 5. Distribution of CS in the Taihang Mountains. Distribution of CS in the Taihang Mountains: (**a**) 1990; (**b**) 2020; (**c**) Scenario A; (**d**) Scenario B; (**e**) Scenario C.

In Scenario C, the overall CS in the Taihang Mountains increased by 18.52 Tg (+1.16%). Forest, shrub, grassland, and water areas experienced significant development; the CS provided by these four types of LUC increased from 1192.41 Tg in 2020 to 1225.04 Tg in 2035 (+2.74%). Specifically, the forested areas demonstrated a rapid expansion, contributing to an additional 40.48 Tg of carbon storage. In contrast, shrub, grassland, and water areas experienced slow contractions, resulting in a collective decrease in carbon storage of 19.039 Tg. The forest type of land cover demonstrated a rapid expansion, contributing to an additional 40.48 Tg of carbon storage. In contrast, shrubs, grasslands, and water each experienced a slow contraction, resulting in a collective decrease of 19.039 Tg in their total CS contribution. Compared to the 2.74% increase in CS, the LUC areas of

these four types only grew by 1.8% from 2020 to 2035. This suggests the significance of developing high-carbon-density types of LUC when enhancing regional carbon storage.

3.3. Spatial Autocorrelation

To investigate the spatial heterogeneity of CS in the Taihang Mountains, the study area was resampled to 1 km, and Moran's I scatterplot (Figure 6) and LISA maps (Figure 7) were used to conduct a spatial autocorrelation analysis of the CS. The results suggest that the distribution of sample points is concentrated in the first and third quadrants, which indicates a clear positive spatial autocorrelation.
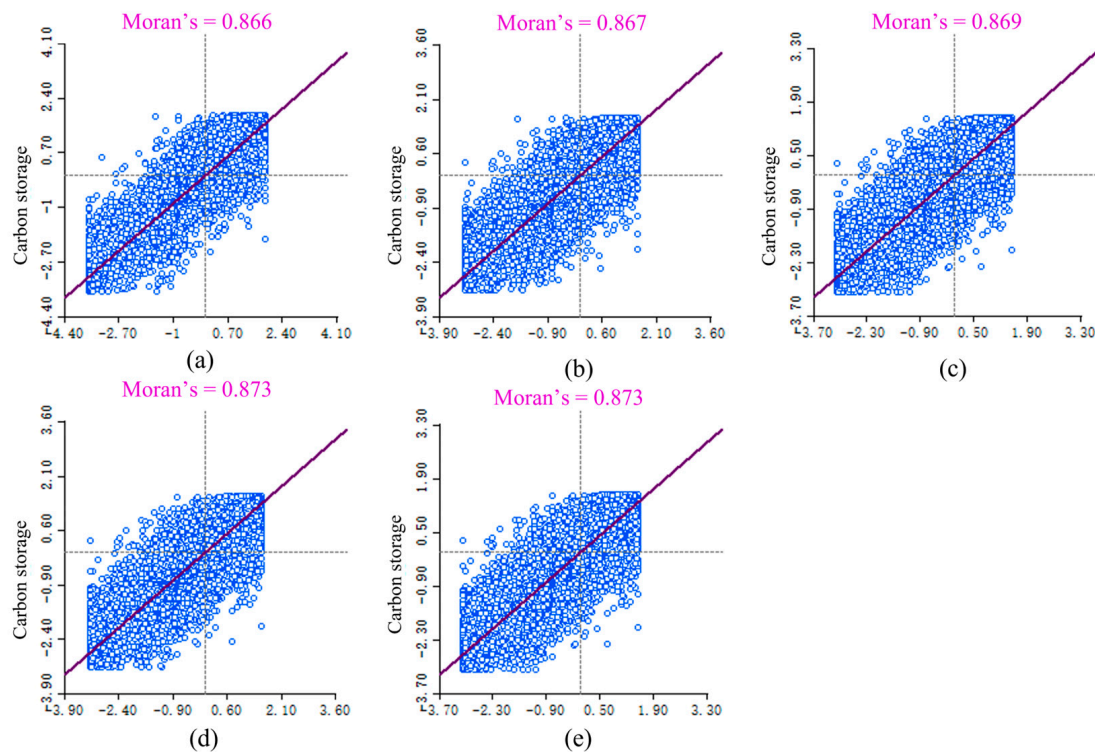
Figure 6. Moran's I scatterplots. Moran's I scatterplots for (**a**) 1990; (**b**) 2020; (**c**) Scenario A; (**d**) Scenario B; (**e**) Scenario C.
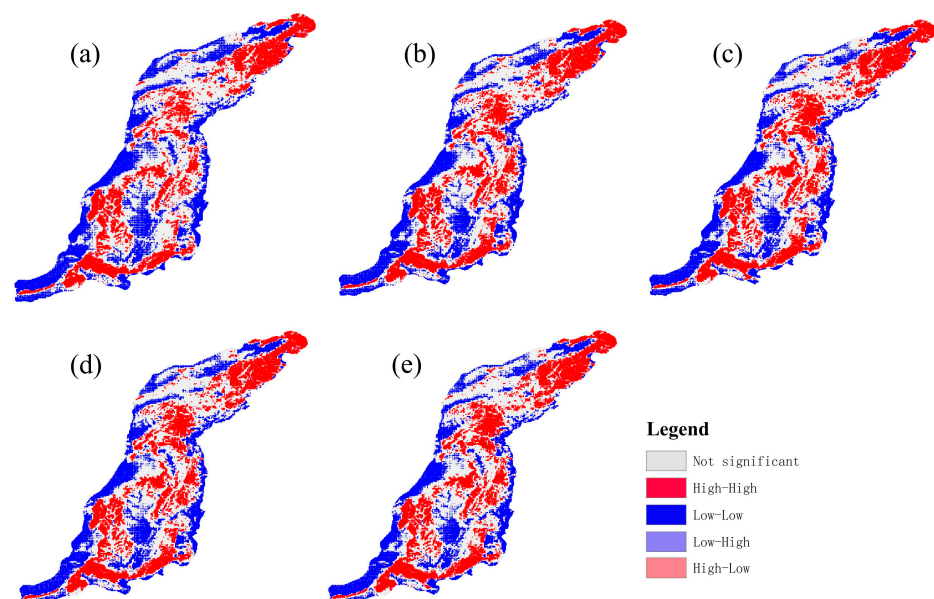
Figure 7. The LISA map. LISA maps for (**a**) 1990; (**b**) 2020; (**c**) Scenario A; (**d**) Scenario B; (**e**) Scenario.

Based on the LISA map (Figure 7), we can observe that low-high aggregation and high-low aggregation are not prominent within the study area. The high–high cluster of carbon storage in the Taihang Mountains is primarily concentrated in the northern and southern mountainous areas, with some distribution in the central mountainous area. However, the concentration in the central area is relatively lower, and the spatial distribution is relatively scattered. On the other hand, the low–low cluster is mainly distributed in the eastern and western plain areas, showing greater overlap with impervious surface areas and agricultural land. In terms of spatial patterns, the high–high cluster exhibits an expanding trend, with its new clusters mainly concentrated in the central mountainous area. This indicates that the increase in CS in the Taihang Mountains is primarily attributed to the improvement in the ecological environment in the central mountainous area. On the contrary, the low–low cluster shows a declining trend which mainly occurs on the northwest edge of the Taihang Mountains, suggesting an improvement in the ecological environment in the Taihang Mountains.

4. Discussions

4.1. The Spatial Conversions of Types of LUC

An ecosystem is a highly complex system, and the study of changes in LUC and CS is a method of understanding the overall ecosystem and its functioning rules. It helps humans to adapt to the natural environment. Based on the LUC transition matrix from 1990 to 2020 in Section 3.1.2, we find that in 1990, there were 7.1118 km^2 of barren land which decreased to 5.49 km^2 by 2020, resulting in a total decline of 22.7%. However, during this period, only 0.5445 km^2 of barren land maintained its original attributes, showing a spatial conversion rate of 92.3%. This high spatial conversion rate of barren land deserves special attention, especially concerning the local ecosystem, as an LUC conversion implies both ecosystem degradation and reconstruction; for environmental protection agencies, such LUC transformations necessitate policy revisions and the reallocation of resources. These factors pose challenges to maintaining ecological stability and policy continuity. This phenomenon is not limited to barren land but extends to other types of LUC to varying degrees. Therefore, in urban planning and the formulation of ecological protection policies, more consideration should be provided to spatial changes in LUC rather than solely focusing on total area changes. Efforts should be made to maintain a relative stability in the spatial distribution of various types of LUC, minimizing frequent human-induced conversions between them. This approach ensures policy continuity, saving costs in societal operations, and fostering a harmonious coexistence between humans and nature [57].

4.2. Analysis of Carbon Storage Changes

We analyzed the impacts of different development scenarios on the LUC and CS in the Taihang Mountains. The results indicate that changes in CS directly reflect changes in LUC [27]. Under the three different development scenarios, the Taihang Mountains exhibit significant spatial heterogeneity in LUC and CS. The types of LUC transitions from high-carbon-density type to low-carbon-density type lead to a reduction in CS, while the transition from low-carbon-density type to high-carbon-density types results in an increase in CS. In the Taihang Mountains, both national and local governments have implemented various measures such as the Taihang Mountain Greening Project and Grain for Green Project. These initiatives have effectively protected the ecological environment of the Taihang Mountains and increased its carbon storage. Considering the intricacies of anthropogenic impacts on the environment and the current advancements in technology, it is generally understood that anthropogenic activities exacerbate carbon emissions, influence the balances of other greenhouse gases, and contribute to regional carbon storage reduction; therefore, strategic policy guidance could potentially yield a favorable role for human activities in regional carbon dynamics. Presently, certain technologies aim to use building materials for carbon storage [58]. Grounded in these technologies, future urban areas might experience significant escalations in carbon density, signifying a constructive implication

for regional carbon storage. Furthermore, due to rough economic development, certain areas have witnessed severe ecological degradation, rendering them unsuitable for human habitation. Therefore, within these areas, the implementation of ecological migration policies could entail relocating local residents and undertaking measures to restore the local ecological environment, consequently heightening regional carbon storage to a certain extent. Meanwhile, in consideration of the highly negative social effects with ecological migration policies [59], our focus should primarily center on supporting the transformation of rural communities in mountainous regions, improving the residents' quality of life and avoiding degradation in the surrounding ecosystem.

4.3. Limitations and Future Perspectives

The PLUS model employs a random forest algorithm to analyze historical LUC data and provides driving factor data to calculate the contributions of different driving factors to changes in various types of LUC. This approach is highly suitable for analyzing historical types of LUC in the study area. However, when simulating future types of LUC, the lack of future relevant driving factors, especially socio-economic factors such as roads, may impact the simulation results. Therefore, in applications, we should strive to obtain the most up-to-date relevant driving factor data and promptly update them to ensure the reliability of the simulation results.

The InVEST model is the most commonly used model for assessing carbon storage. It offers unique advantages, such as lower data requirements, less intensive computations, and higher accuracy in drawing conclusions. However, it is not without its limitations. When calculating carbon storage, the InVEST model relies on types of LUC combined with their respective carbon density values. This approach overlooks the impact of vegetation types and their growth cycles on carbon density within the same LUC type. Alterations in vegetation types are influenced by a multitude of factors, whereas in regions characterized by intensive human activities, these alterations are primarily shaped by policies and management practices. Additionally, the carbon density of the same vegetation type can vary in different regions due to local environmental influences. Under diverse climatic circumstances, the growth status of identical plants can significantly vary, consequently impacting their carbon sequestration capacities and subsequently affecting regional carbon densities. In summary, the influences of factors such as vegetation type, soil type, and climate change on carbon storage are dynamic, which the InVEST model does not consider. In future research, it is advisable to collect field data on carbon density for various vegetation types within a study area. Combining these data with predictive models can enhance the accuracy of future carbon storage assessments.

5. Conclusions

We utilized the PLUS and InVEST models to simulate and analyze changes in LUC and their impact on CS in the region of the Taihang Mountains from 1990 to 2035 for three different development scenarios. The results show a strong correlation between overall carbon storage changes and forest carbon storage [11]. In Scenario A, the carbon storage in the Taihang Mountains gradually increases. In Scenario B, croplands expand significantly, while forests and local economic development are constrained. Compared to Scenario A, the forests decrease by 1.5% and the impervious surfaces decrease by 11.7%. In this scenario, the expansion of cropland becomes the primary driver for the increase in carbon storage in the study area. In Scenario C, forests experience the most significant development, leading to the highest overall carbon storage among the three scenarios. Carbon storage changes in the Taihang Mountains mainly occur in the central mountainous areas and areas adjacent to forests in different scenarios, indicating their sensitivity and the need for more attention from the relevant planning and environmental protection departments. Our study precisely identifies transitions in land cover type and their impact on carbon storage in these sensitive areas, providing valuable insights for relevant environmental policies and urban development planning.

References

1. Sun, L.; Yu, H.; Sun, M.; Wang, Y. Coupled Impacts of Climate and Land Use Changes on Regional Ecosystem Services. *J. Environ. Manag.* **2023**, *326*, 116753. [CrossRef] [PubMed]
2. Li, J.; Chen, X.; Kurban, A.; Van de Voorde, T.; De Maeyer, P.; Zhang, C. Coupled SSPs-RCPs Scenarios to Project the Future Dynamic Variations of Water-Soil-Carbon-Biodiversity Services in Central Asia. *Ecol. Indic.* **2021**, *129*, 107936. [CrossRef]
3. Fu, H.-Z.; Waltman, L. A Large-Scale Bibliometric Analysis of Global Climate Change Research between 2001 and 2018. *Clim. Chang.* **2022**, *170*, 36. [CrossRef]
4. Shen, L.; Zeng, Q. Multiscenario Simulation of Land Use and Land Cover in the Zhundong Mining Area, Xinjiang, China. *Ecol. Indic.* **2022**, *145*, 109608. [CrossRef]
5. Chen, Y.; Yan, H.; Yao, Y.; Zeng, C.; Gao, P.; Zhuang, L.; Fan, L.; Ye, D. Relationships of Ozone Formation Sensitivity with Precursors Emissions, Meteorology and Land Use Types, in Guangdong-Hong Kong-Macao Greater Bay Area, China. *J. Environ. Sci.* **2020**, *94*, 1–13. [CrossRef]
6. Kertész, Á.; Nagy, L.A.; Balázs, B. Effect of Land Use Change on Ecosystem Services in Lake Balaton Catchment. *Land Use Policy* **2019**, *80*, 430–438. [CrossRef]
7. Guo, W.; Teng, Y.; Yan, Y.; Zhao, C.; Zhang, W.; Ji, X. Simulation of Land Use and Carbon Storage Evolution in Multi-Scenario: A Case Study in Beijing-Tianjin-Hebei Urban Agglomeration, China. *Sustainability* **2022**, *14*, 13436. [CrossRef]
8. Kantzas, E.P.; Val Martin, M.; Lomas, M.R.; Eufrasio, R.M.; Renforth, P.; Lewis, A.L.; Taylor, L.L.; Mecure, J.-F.; Pollitt, H.; Vercoulen, P.V.; et al. Substantial Carbon Drawdown Potential from Enhanced Rock Weathering in the United Kingdom. *Nat. Geosci.* **2022**, *15*, 382–389. [CrossRef]
9. Liu, C.; Zhang, X.; Wang, T.; Chen, G.; Zhu, K.; Wang, Q.; Wang, J. Detection of Vegetation Coverage Changes in the Yellow River Basin from 2003 to 2020. *Ecol. Indic.* **2022**, *138*, 108818. [CrossRef]
10. Zhou, Z.; Sun, X.; Zhang, X.; Wang, Y. Inter-Regional Ecological Compensation in the Yellow River Basin Based on the Value of Ecosystem Services. *J. Environ. Manag.* **2022**, *322*, 116073. [CrossRef]
11. Luby, I.H.; Miller, S.J.; Polasky, S. When and Where to Protect Forests. *Nature* **2022**, *609*, 89–93. [CrossRef] [PubMed]
12. Forzieri, G.; Girardello, M.; Ceccherini, G.; Spinoni, J.; Feyen, L.; Hartmann, H.; Beck, P.S.A.; Camps-Valls, G.; Chirici, G.; Mauri, A.; et al. Emergent Vulnerability to Climate-Driven Disturbances in European Forests. *Nat. Commun.* **2021**, *12*, 1081. [CrossRef] [PubMed]
13. Lai, L.; Huang, X.; Yang, H.; Chuai, X.; Zhang, M.; Zhong, T.; Chen, Z.; Chen, Y.; Wang, X.; Thompson, J.R. Carbon Emissions from Land-Use Change and Management in China between 1990 and 2010. *Sci. Adv.* **2016**, *2*, e1601063. [CrossRef] [PubMed]
14. Liu, W.; Zhan, J.; Zhao, F.; Yan, H.; Zhang, F.; Wei, X. Impacts of Urbanization-Induced Land-Use Changes on Ecosystem Services: A Case Study of the Pearl River Delta Metropolitan Region, China. *Ecol. Indic.* **2019**, *98*, 228–238. [CrossRef]
15. Zhang, Y.; Long, H.; Tu, S.; Ge, D.; Ma, L.; Wang, L. Spatial Identification of Land Use Functions and Their Tradeoffs/Synergies in China: Implications for Sustainable Land Management. *Ecol. Indic.* **2019**, *107*, 105550. [CrossRef]
16. Zhou, W.; Yu, W.; Qian, Y.; Han, L.; Pickett, S.T.A.; Wang, J.; Li, W.; Ouyang, Z. Beyond City Expansion: Multi-Scale Environmental Impacts of Urban Megaregion Formation in China. *Natl. Sci. Rev.* **2022**, *9*, nwab107. [CrossRef] [PubMed]
17. Peng, J.; Tian, L.; Zhang, Z.; Zhao, Y.; Green, S.M.; Quine, T.A.; Liu, H.; Meersmans, J. Distinguishing the Impacts of Land Use and Climate Change on Ecosystem Services in a Karst Landscape in China. *Ecosyst. Serv.* **2020**, *46*, 101199. [CrossRef]
18. Mendoza-Ponce, A.; Corona-Núñez, R.O.; Nava, L.F.; Estrada, F.; Calderón-Bustamante, O.; Martínez-Meyer, E.; Carabias, J.; Larralde-Corona, A.H.; Barrios, M.; Pardo-Villegas, P.D. Impacts of Land Management and Climate Change in a Developing and Socioenvironmental Challenging Transboundary Region. *J. Environ. Manag.* **2021**, *300*, 113748. [CrossRef]
19. Yang, Q.; Liu, G.; Casazza, M.; Dumontet, S.; Yang, Z. Ecosystem Restoration Programs Challenges under Climate and Land Use Change. *Sci. Total Environ.* **2022**, *807*, 150527. [CrossRef]

20. Nie, X.; Lu, B.; Chen, Z.; Yang, Y.; Chen, S.; Chen, Z.; Wang, H. Increase or Decrease? Integrating the CLUMondo and InVEST Models to Assess the Impact of the Implementation of the Major Function Oriented Zone Planning on Carbon Storage. *Ecol. Indic.* **2020**, *118*, 106708. [CrossRef]

21. Wang, H.; Wu, X.; Wu, D.; Nie, X. Will Land Development Time Restriction Reduce Land Price? The Perspective of American Call Options. *Land Use Policy* **2019**, *83*, 75–83. [CrossRef]

22. Yu, H.; Xie, W.; Sun, L.; Wang, Y. Identifying the Regional Disparities of Ecosystem Services from a Supply-Demand Perspective. *Resour. Conserv. Recycl.* **2021**, *169*, 105557. [CrossRef]

23. Tao, Y.; Tian, L.; Wang, C.; Dai, W. Dynamic Simulation of Land Use and Land Cover and Its Effect on Carbon Storage in the Nanjing Metropolitan Circle under Different Development Scenarios. *Front. Ecol. Evol.* **2023**, *11*, 1102015. [CrossRef]

24. Aneseyee, A.B.; Soromessa, T.; Elias, E.; Noszczyk, T.; Hernik, J.; Benti, N.E. Expressing Carbon Storage in Economic Terms: The Case of the Upper Omo Gibe Basin in Ethiopia. *Sci. Total Environ.* **2022**, *808*, 152166. [CrossRef]

25. Ostle, N.J.; Levy, P.E.; Evans, C.D.; Smith, P. UK Land Use and Soil Carbon Sequestration. *Land Use Policy* **2009**, *26*, S274–S283. [CrossRef]

26. Wasige, J.E.; Groen, T.A.; Rwamukwaya, B.M.; Tumwesigye, W.; Smaling, E.M.A.; Jetten, V. Contemporary Land Use/Land Cover Types Determine Soil Organic Carbon Stocks in South-West Rwanda. *Nutr. Cycl. Agroecosyst.* **2014**, *100*, 19–33. [CrossRef]

27. Zhao, M.; He, Z.; Du, J.; Chen, L.; Lin, P.; Fang, S. Assessing the Effects of Ecological Engineering on Carbon Storage by Linking the CA-Markov and InVEST Models. *Ecol. Indic.* **2019**, *98*, 29–38. [CrossRef]

28. Hersperger, A.M.; Oliveira, E.; Pagliarin, S.; Palka, G.; Verburg, P.; Bolliger, J.; Grădinaru, S. Urban Land-Use Change: The Role of Strategic Spatial Planning. *Glob. Environ. Chang.* **2018**, *51*, 32–42. [CrossRef]

29. Zhang, S.; Yang, P.; Xia, J.; Wang, W.; Cai, W.; Chen, N.; Hu, S.; Luo, X.; Li, J.; Zhan, C. Land Use/Land Cover Prediction and Analysis of the Middle Reaches of the Yangtze River under Different Scenarios. *Sci. Total Environ.* **2022**, *833*, 155238. [CrossRef]

30. Zhu, W.; Zhang, J.; Cui, Y.; Zhu, L. Ecosystem Carbon Storage under Different Scenarios of Land Use Change in Qihe Catchment, China. *J. Geogr. Sci.* **2020**, *30*, 1507–1522. [CrossRef]

31. Kulaixi, Z.; Chen, Y.; Li, Y.; Wang, C. Dynamic Evolution and Scenario Simulation of Ecosystem Services under the Impact of Land-Use Change in an Arid Inland River Basin in Xinjiang, China. *Remote Sens.* **2023**, *15*, 2476. [CrossRef]

32. Lang, Y.; Song, W. Quantifying and Mapping the Responses of Selected Ecosystem Services to Projected Land Use Changes. *Ecol. Indic.* **2019**, *102*, 186–198. [CrossRef]

33. Xiao, Y.; Huang, M.; Xie, G.; Zhen, L. Evaluating the Impacts of Land Use Change on Ecosystem Service Values under Multiple Scenarios in the Hunshandake Region of China. *Sci. Total Environ.* **2022**, *850*, 158067. [CrossRef] [PubMed]

34. Wang, P.; Yu, P.; Lu, J.; Zhang, Y. The Mediation Effect of Land Surface Temperature in the Relationship between Land Use-Cover Change and Energy Consumption under Seasonal Variations. *J. Clean. Prod.* **2022**, *340*, 130804. [CrossRef]

35. He, Y.; Ma, J.; Zhang, C.; Yang, H. Spatio-Temporal Evolution and Prediction of Carbon Storage in Guilin Based on FLUS and InVEST Models. *Remote Sens.* **2023**, *15*, 1445. [CrossRef]

36. Zhu, G.; Qiu, D.; Zhang, Z.; Sang, L.; Liu, Y.; Wang, L.; Zhao, K.; Ma, H.; Xu, Y.; Wan, Q. Land-Use Changes Lead to a Decrease in Carbon Storage in Arid Region, China. *Ecol. Indic.* **2021**, *127*, 107770. [CrossRef]

37. Liu, Q.; Yang, D.; Cao, L.; Anderson, B. Assessment and Prediction of Carbon Storage Based on Land Use/Land Cover Dynamics in the Tropics: A Case Study of Hainan Island, China. *Land* **2022**, *11*, 244. [CrossRef]

38. Wang, Z.; Li, X.; Mao, Y.; Li, L.; Wang, X.; Lin, Q. Dynamic Simulation of Land Use Change and Assessment of Carbon Storage Based on Climate Change Scenarios at the City Level: A Case Study of Bortala, China. *Ecol. Indic.* **2022**, *134*, 108499. [CrossRef]

39. Zheng, H.; Zheng, H. Assessment and Prediction of Carbon Storage Based on Land Use/Land Cover Dynamics in the Coastal Area of Shandong Province. *Ecol. Indic.* **2023**, *153*, 110474. [CrossRef]

40. Xu, C.; Zhang, Q.; Yu, Q.; Wang, J.; Wang, F.; Qiu, S.; Ai, M.; Zhao, J. Effects of Land Use/Cover Change on Carbon Storage between 2000 and 2040 in the Yellow River Basin, China. *Ecol. Indic.* **2023**, *151*, 110345. [CrossRef]

41. Ma, A.; He, N.; Yu, G.; Wen, D.; Peng, S. Carbon Storage in Chinese Grassland Ecosystems: Influence of Different Integrative Methods. *Sci. Rep.* **2016**, *6*, 21378. [CrossRef] [PubMed]

42. Wu, W.; Xu, L.; Zheng, H.; Zhang, X. How Much Carbon Storage Will the Ecological Space Leave in a Rapid Urbanization Area? Scenario Analysis from Beijing-Tianjin-Hebei Urban Agglomeration. *Resour. Conserv. Recycl.* **2023**, *189*, 106774. [CrossRef]

43. Chanapathi, T.; Thatikonda, S. Investigating the Impact of Climate and Land-Use Land Cover Changes on Hydrological Predictions over the Krishna River Basin under Present and Future Scenarios. *Sci. Total Environ.* **2020**, *721*, 137736. [CrossRef] [PubMed]

44. Zellweger, F.; Flack-Prain, S.; Footring, J.; Wilebore, B.; Willis, K.J. Carbon Storage and Sequestration Rates of Trees inside and Outside Forests in Great Britain. *Environ. Res. Lett.* **2022**, *17*, 074004. [CrossRef]

45. Gao, L.; Tao, F.; Liu, R.; Wang, Z.; Leng, H.; Zhou, T. Multi-Scenario Simulation and Ecological Risk Analysis of Land Use Based on the PLUS Model: A Case Study of Nanjing. *Sustain. Cities Soc.* **2022**, *85*, 104055. [CrossRef]

46. Meimei, W.; Zizhen, J.; Tengbiao, L.; Yongchun, Y.; Zhuo, J. Analysis on Absolute Conflict and Relative Conflict of Land Use in Xining Metropolitan Area under Different Scenarios in 2030 by PLUS and PFCI. *Cities* **2023**, *137*, 104314. [CrossRef]

47. Fang, Z.; Ding, T.; Chen, J.; Xue, S.; Zhou, Q.; Wang, Y.; Wang, Y.; Huang, Z.; Yang, S. Impacts of Land Use/Land Cover Changes on Ecosystem Services in Ecologically Fragile Regions. *Sci. Total Environ.* **2022**, *831*, 154967. [CrossRef]

48. Zhang, X.; Liu, K.; Wang, S.; Wu, T.; Li, X.; Wang, J.; Wang, D.; Zhu, H.; Tan, C.; Ji, Y. Spatiotemporal Evolution of Ecological Vulnerability in the Yellow River Basin under Ecological Restoration Initiatives. *Ecol. Indic.* **2022**, *135*, 108586. [CrossRef]

49. Huang, A.; Xu, Y.; Sun, P.; Zhou, G.; Liu, C.; Lu, L.; Xiang, Y.; Wang, H. Land Use/Land Cover Changes and Its Impact on Ecosystem Services in Ecologically Fragile Zone: A Case Study of Zhangjiakou City, Hebei Province, China. *Ecol. Indic.* **2019**, *104*, 604–614. [CrossRef]

50. Wang, K.; Li, X.; Lyu, X.; Dang, D.; Dou, H.; Li, M.; Liu, S.; Cao, W. Optimizing the Land Use and Land Cover Pattern to Increase Its Contribution to Carbon Neutrality. *Remote Sens.* **2022**, *14*, 4751. [CrossRef]

51. Yang, J.; Huang, X. The 30 m Annual Land Cover Dataset and Its Dynamics in China from 1990 to 2019. *Earth Syst. Sci. Data* **2021**, *13*, 3907–3925. [CrossRef]

52. Liang, X.; Guan, Q.; Clarke, K.C.; Liu, S.; Wang, B.; Yao, Y. Understanding the Drivers of Sustainable Land Expansion Using a Patch-Generating Land Use Simulation (PLUS) Model: A Case Study in Wuhan, China. *Comput. Environ. Urban Syst.* **2021**, *85*, 101569. [CrossRef]

53. Koenig, W.D. Spatial Autocorrelation of Ecological Phenomena. *Trends Ecol. Evol.* **1999**, *14*, 22–26. [CrossRef] [PubMed]

54. Anselin, L. The Moran Scatterplot as an ESDA Tool to Assess Local Instability in Spatial Association. In *Spatial Analytical Perspectives on GIS*; Routledge: London, UK, 1996; ISBN 978-0-203-73905-1.

55. Anselin, L. Local Indicators of Spatial Association—LISA. *Geogr. Anal.* **1995**, *27*, 93–115. [CrossRef]

56. Cohen, J. A Coefficient of Agreement for Nominal Scales. *Educ. Psychol. Meas.* **1960**, *20*, 37–46. [CrossRef]

57. Dong, X.; Ren, J.; Zhang, P.; Jin, Y.; Liu, R.; Wang, X.-C.; Lee, C.T.; Klemeš, J.J. Entwining Ecosystem Services, Land Use Change and Human Well-Being by Nitrogen Flows. *J. Clean. Prod.* **2021**, *308*, 127442. [CrossRef]

58. Buildings as a Global Carbon Sink | Nature Sustainability. Available online: https://www.nature.com/articles/s41893-019-0462-4 (accessed on 24 August 2023).

59. Hu, Y.; Zhou, W.; Yuan, T. Environmental Impact Assessment of Ecological Migration in China: A Survey of Immigrant Resettlement Regions. *J. Zhejiang Univ. Sci. A* **2018**, *19*, 240–254. [CrossRef]